CHEMICAL ENGINEERING TRANSACTIONS

VOL. 103, 2023

A publication of AIDIC
The Italian Association of Chemical Engineering
Online at www.cetjournal.it

Guest Editors: Petar S. Varbanov, Panos Seferlis, Yee Van Fan, Athanasios Papadopoulos

ISBN 979-12-81206-02-1; **ISSN** 2283-9216

DOI: 10.3303/CET23103089

Integrated Renewable Energy and Polygeneration Hub Design for Industrial Heat and Power Utilisation

Takudzwa B. Chitsiga, Adeniyi J. Isafiade*

Department of Chemical Engineering, Universty of Cape Town Rondebosch, 7701, South Africa
niyi.isafiade@uct.ac.za

This paper outlines the development of an integrated resource network that comprises an energy supply chain, a polygeneration hub for combined heat, power, and absorption refrigeration system, to meet demand for heating, cooling, and electricity generation. The method adopted involves a 3-layered superstructure where the first layer comprises a supply chain network of seasonal renewable and non-renewable energy sources which are connected to the second layer through transport modes such as rail, road, and pipeline. The second layer comprises the polygeneration hub which plays host to technologies such as a boiler for generating high pressure steam, turbines for generating power, and an absorption refrigeration system for water cooling. The third layer of the superstructure, which is connected to the second layer through pipelines and transmission cables, comprises the heat exchanger network of a process plant. The solution of the developed model, which is a mixed integer non-linear program, is evaluated using economics and environmental impact and is solved using the goal method of multi-objective optimisation. In the hypothetical case study investigated, the model showed a higher preference for renewable energy when environmental impact was considered as the only objective to be minimised, while coal was selected when economics was the only objective minimised and when both objectives were simultaneously minimised with an equal weighting. In addition, the cost minimisation scenario resulted in fewer heat exchangers being selected than in the environmental and multi-objective optimisation scenarios.

1. Introduction

Climate change has become an urgent global issue, requiring a shift towards sustainable practices to mitigate its impacts. This shift includes optimisation of energy networks, including utilities, as well as increased use of renewable energy sources. The reduction of greenhouse gas (GHG) emissions is crucial but must be balanced with cost-effectiveness. Several studies have shown methods to integrate renewable energy with power and heat generation. Cowen et al. (2019) integrated a bioenergy supply chain network with the multiperiod heat demand of three co-located process plants. Isafiade and Short (2022) developed an integrated energy network that included a bioenergy supply chain, combined heat and power generation, and heat exchanger network (HEN). Although the objective criteria adopted by the authors is Total Annual Cost (TAC), however, capital costs for the boiler and turbines at the energy hub were not included. Also, the benefits associated with including absorption refrigeration in the integrated network was not explored. Isafiade et al. (2022) extended the work of Cowen et al. (2019) by considering interplant heat integration using the energy hub approach. Sun et al. (2019) integrated an absorption refrigeration cycle with a HEN with the aim of simultaneously optimising their operating parameters. However, no consideration was given to the benefits of integrating multiple sources of energy with their network. Xu et al. (2022) proposed an integrated energy system which combined solar and geothermal energy with a multi-objective function that considered the economic, energy and environmental performance but also did not include in their network consideration for multiple sources of energy for the utilities using the supply chain model. The aim of this research paper is to develop a model for a polygeneration hub that is integrated with a supply chain network (SCN) of renewable and non-renewable energy sources. The polygeneration hub, which will include a boiler for steam generation, turbines for power generation and an absorption refrigeration system, will supply hot and cold utilities, as well as power, to nearby industrial demand

Paper Received: 02 May 2023; Revised: 21 June 2023; Accepted: 27 July 2023
Please cite this article as: Chitsiga T.B., Isafiade A.J., 2023, Integrated Renewable Energy and Polygeneration Hub Design for Industrial Heat and Power Utilisation, Chemical Engineering Transactions, 103, 529-534 DOI:10.3303/CET23103089

nodes. The model will also simultaneously account for the environmental impact of the transportation and combustion of energy feedstocks in the boiler and the TAC of the overall integrated network, including detailed equipment costing.

2. Problem statement

This paper addresses the following problem. Given a set of biomass energy sources sp, that can supply feedstock to be transported by a set of freight modes f, to a polygeneration hub located at a distance D from the supply points. Each feedstock has a seasonal availability, denoted by the set s, and associated unit costs. The polygeneration hub is required to produce heating and cooling utilities to satisfy heat demand by a set of hot H and cold C process streams that have specified heat capacity flowrates FCP and heat transfer coefficients h. An absorption refrigeration system (ARS), which is a subnetwork of the polygeneration hub, comprises a set of units denoted by ars. Additional parameters given in the problem include transport costs for the energy feedstocks, heat exchanger installation and area costs, and unit-based costs for the utilities. The aim is to design an integrated network that optimally distributes resources and energy to satisfy demand for heat and electricity considering both economic and environmental objectives.

3. Methodology

Figure 1 is the superstructure that describes the proposed integrated resource network. The SCN of renewable energy feedstocks is shown in the first layer and is connected through freight modes to the second layer, which comprises the power generation units and the ARS that requires hot utility. The third layer consists of a process plant that requires hot and cold utilities and specified electricity demand. It is assumed that the second layer is connected to the third layer by utility pipes and power cables. The mathematical model for this superstructure is represented and solved as a Mixed Integer Non-Linear Program (MINLP). This paper differs from that of Isafiade and Short (2022) in that it considered the emissions derived from the transportation of feedstocks, and data for transport factors is obtained from the literature. Also, in this paper, the polygeneration subnetwork which includes an ARS network, uses values obtained from Towler and Sinnott (2022) to cost the boiler and turbines. This is unlike the model of Isafiade and Short (2022) that only accounted for the operating costs of their energy hub which did not include an ARS network. The ARS model of this paper is adapted from Florides et al. (2003) and is based on a single stage lithium bromide ARS with four major units, the generator, condenser, evaporator, and absorber. But the model differs from that of Florides et al. (2003) in that it is connected to the excess low-pressure steam (LPS) exiting the turbine of the power generation unit after it has been desuperheated. The ARS model of this paper is also connected to the cold utility demand of the HEN model of the overall network. This implies that the LPS exiting the turbine serves as heat source to drive the refrigeration cycle in the ARS, while the ARS evaporator provides cooling to satisfy demand for cold utility by the HEN of the process plant.

The overall model has a multi-objective function which comprises the economic objective and environmental objective. The economic objective sums up the annual operating and capital costs for the SCN, polygeneration network and the HEN. The environmental objective comprises the carbon emissions by virtue of shipping the feedstocks within the SCN as well as their combustion in the boiler in the polygeneration hub. Eq (1) shows the economic objective function.

$$Min\ \dot{T}AC = \left\{ \sum_{sp \in SP} \sum_{f \in F} \sum_{s \in S} TSCN_{sp,f,S} \right\} + WTC + \mathrm{AF} \cdot (Bcst + TBcst + HENcst + ARScst) + \{(0.0239 * PP * OH) + (0.00983 * EP * OH)\} \quad (1)$$

In Eq(1), the first term on the right-hand side $TSCN_{sp,f,s}$, is the total annual supply chain network cost. WTC is the total cost of water used in the power generation subnetwork, Bcst, TBcst, HENcst and ARScst are the capital costs for boiler, turbine, HEN, and ARS installations. AF is an annualization factor calculated from specified discount rates. The ARS subnetwork is modelled as a set of heat exchangers. In Eq(1), 0.0239 \$/(kW·h) is the unit cost of purchased power PP, 0.00983 \$/(kW·h) is the unit cost of the penalty for unused excess power EP, while OH is the number of annual operating hours (8,160 h). According to the work of Edgar et al., from which the material and energy balances, including data, for the turbines were obtained, if the power produced by the turbines is insufficient to meet the demand, then additional power, PP, can be purchased with the minimum being 12,000 kW. However, if this minimum power is not fully utilized, then penalty charges will be incurred for the excess unused power, EP. Eq(2) shows the environmental objective which comprises the mass flow rate of emissions from the boiler (EmB) in kg/y summed over all the feedstock supply points, and the emissions from the transportation of feedstocks (EmT) in kg/y summed over all the modes of transport. The calculation of EmB is like that of Isafiade and Short (2022). EmT is calculated by multiplying the mass of feedstock (kg) by the distance traveled from the supply point (km) and by the emission factor (gCO_2/t-km). The expression is then divided by 10^6 to convert the obtained mass of CO_2 from grams to kg.

$$Min\dot{EI} = \sum_{sp \in SP} EmB + \sum_{f \in F} EmT \quad (2)$$

This calculation is done for all supply points and seasons of feedstock availability. The emission factors are obtained from IFEU (2008). This paper adopts the method of weighted sum multi-objective optimisation shown in Eq(3) as used by Isafiade and Short (2022). In Eq(3), MO is the multi-objective variable and R_g is the weighting factor.

$$Min\dot{MO} = R_g \cdot \left(\frac{TAC}{TAC_{min}}\right) + (1 - R_g) \cdot \left(\frac{EI}{EI_{min}}\right) \quad (3)$$

4. Case study

The case study to which the model was applied has four feedstocks: sewage sludge, forestry residue, biogas, and coal. Each renewable feedstock is located at a certain distance from the polygeneration hub and has varying costs and availability over 3 different agricultural seasons as shown in Table 1. NCV is the net calorific value of each feedstock expressed in kWh/kg. Over all the seasons, coal serves as a supplementary fuel in the event of insufficient renewable fuel sources. Table 2 shows the different modes of transport available and their respective cost parameters and scaling factors. AF is the annualization factor for investment cost on the transport network, T_f^{FC} and T_f^{VC} are the fixed and variable costs associated with transportation. T_f^{IC} is the investment cost for the transportation network, τ_f is the tortuosity factor accounting for route curvature in the network and t_{RF} is the return trip factor which accounts for return trip distance to the supply points. The HEN in the hypothetical process plant has 2 hot process streams and 4 cold process streams. As shown in Figure 1, the hot utilities are LPS and medium-pressure steam (MPS) that exit the two turbines in the polygeneration hub and a split branch of the HPS flowing directly from the boiler to the HEN. The LPS stream is split, and part of it feeds into the generator of the ARS subnetwork while the other branch flows into the HEN. The cold utility for the HEN is provided by the ARS evaporator. The ARS condenser and absorber are assumed to be connected to a cooling system with a cooling tower. As shown in Figure 1, the connection between the polygeneration hub and the HEN comprises these hot and cold utility streams. The properties of the streams in the process plant are shown in Table 3. The initial input parameters of the ARS are shown in Table 4, where the evaporator liquid carryover is assumed to be 2.5 % of the vapor leaving the evaporator (m_{10}), which is a variable.

Table 1: Supply chain feedstock data

Feedstock		Season 1		Season 2		Season 3	
	NCV (kWh/kg)	Cost ($/kg)	Capacity (×10^6 kg)	Cost ($/kg)	Capacity (×10^6 kg)	Cost ($/kg)	Capacity (×10^6 kg)
Sewage sludge	4.52	0.024	3	0.022	4.5	0.027	2
Forestry residue	4.95	0.040	250	0.045	210	0.025	30
Biogas	5.08	0.050	450	0.03	500	0.07	2,000
Coal	7.20	0.900	50	0.9	50	0.9	50

Table 2: Supply chain transport data (adapted from Cowen et al., 2019)

Transport mode			Transport parameter			
	AF	T_f^{FC}($/t·km)	T_f^{VC}($/km)	T_f^{IC}($/t·km)	τ_f	t_{RF}
Truck	0.20	0.002	0.0900	5,000	1.27	2
Railway	0.25	0.005	0.0070	50,000	1.10	2
Pipeline	0.50	0.000	0.0001	1.5×10^5	1.27	1

AF in Table 2 is calculated from the discount rates 10 %, 15 % and 23 % for road, railway, and pipeline, whilst annualization is done over 10 y, 7 y, and 3 y. A discount rate of 30 % was used for the heat exchangers, boiler, and turbines over 10 y. The streams in the HEN were assumed to have a uniform heat transfer coefficient of 0.5 (kW/(m^2·℃)) whilst the ARS heat transfer coefficients of 0.85, 1.50, 1.10, 0.85, and 1.40 (kW/(m^2·℃)) for the absorber, evaporator, solution heat exchanger, generator and condenser were derived from DiPippo (2008). To ensure maximum heating efficiency, the HPS leaving the boiler and the MPS and LPS from the turbines were desuperheated by addition of water using calculations from Wen (2020).

Table 3: Process plant's HEN stream data (adapted from Isafiade and Short (2022))

Hot streams	T_i^s (°C)	T_i^t (°C)	FCP_i (kW/°C)	Cold streams	T_j^s (°C)	T_j^t (°C)	FCP_j (kW/°C)
HU1 (HPS)	257	257	-	C1	25	240	140
HU2 (MPS)	197	197	-	C2	20	250	150
HU3 (LPS)	150	150	-	C3	50	180	70
H1	155	85	150	C4	70	100	120
H2	230	40	285	CU1	6.5	10	-

Table 4: ARS subnetwork input parameters

Parameter	Symbol	Input Value
Capacity	Q_{evap}	40 kW
Evaporator Temperature	T_{10}	6 °C
Exit temperature of generator solution	T_4	90 ℃
Mass fraction of weak solution	x_1	55 % LiBr
Mass fraction of strong solution	x_4	60 % LiBr
Exit temperature of solution heat exchanger	T_3	65 °C
Generator vapor exit temperature	T_7	85 °C
Evaporator liquid carryover	m_{11}	0.025 m_{10}

Table 5: Solutions to significant model variables

Scenarios	TAC ($\times 10^8$ $)	EI ($\times 10^{11}$ kg/y)	HEs	Feedstock	Transport mode	Feedstock quantity (kW)
1st (TAC_{min})	5.24	1.03	10	Forestry residue	Railway	13,649
				Sewage sludge	Road	831
				Sewage sludge	Railway	3,947
				Biogas	Road	61,818
				Biogas	Railway	270,173
				Biogas	Pipeline	536,952
				Coal	Railway	3,309
2nd (EI_{min})	11.0	0.00095	16	Forestry residue	Road	67,886
				Forestry residue	Railway	222,931
				Sewage sludge	Railway	3,947
				Sewage sludge	Road	3,947
				Biogas	Road	48,886
				Biogas	Railway	93,382
				Biogas	Pipeline	441,052
3rd (Multi-objective)	5.42	0.00098	17	Forestry residue	Road	187,248
				Sewage sludge	Railway	3,947
				Sewage sludge	Road	831
				Biogas	Road	60,451
				Biogas	Railway	93,382
				Biogas	Pipeline	443,570
				Coal	Railway	3,309

The integrated MINLP model was solved in General Algebraic Modelling System (GAMS) environment (GAMS development corporation, 2015), using DICOPT solver on an 11th Gen Intel(R) Core (TM) i5-1135G7 @ 2.40GHz processor. The model comprised 483 equations, 363 variables and 50 discrete variables. The solution approach adopted involves the simultaneous optimisation of the three layers of the superstructure. Variables such as heat exchanger heat loads and approach temperatures, the HEN intermediate temperature values, flowrates and enthalpy of the streams in the ARS subnetwork of Figure 1 were initialised. 3 scenarios were investigated to implement the multi-objective weighting shown in Eq(3). The first scenario minimized only the TAC as the objective function, leaving the EI unbounded, resulting in a TAC_{min} of 5.24 × 10^8 $ and EI of 1.03 × 10^{11} kg/y. The second scenario minimized only the EI, leaving TAC unbounded and resulting in an EI_{min} of 9.48 × 10^7 kg/y and TAC of 1.1 × 10^9 $. The third scenario investigated included the multi-objective function with an equal weighting (R_g = 0.5) allocated to EI and TAC objectives. For this scenario, an EI value of 9.8 × 10^7 kg/y and TAC of 5.42 × 10^8 $ was obtained. Table 5 shows the solutions for key variables obtained for the 3 scenarios investigated. In the table, HE refers to the number of heat exchangers in the HEN, and the quantity of each feedstock transported by a specific transport mode over a year is shown in the last column.

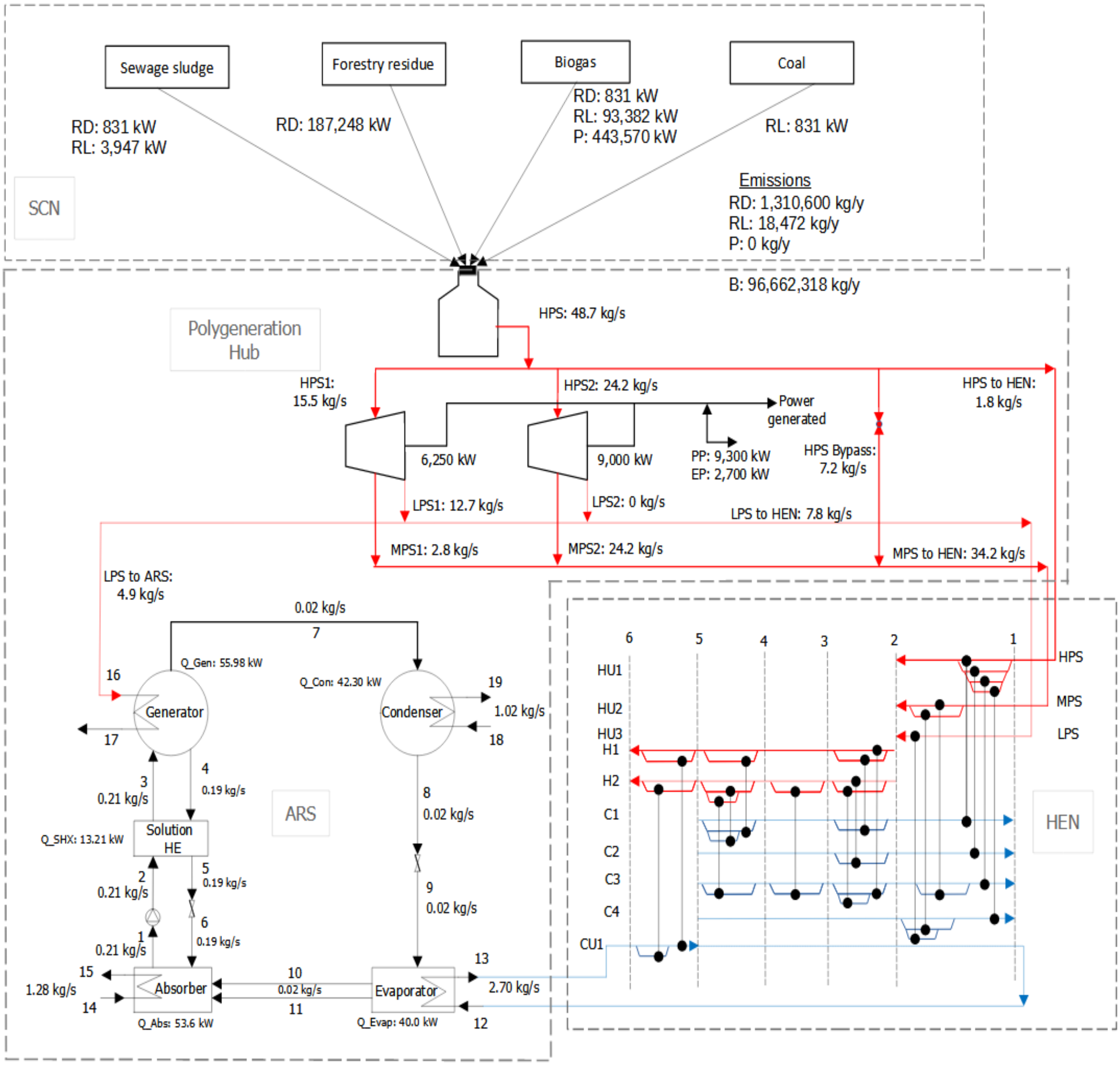

Figure 1: Superstructure illustrating the integrated SCN, polygeneration network and HEN case study

From Table 5, where TAC is constrained, the model minimizes the number of heat exchangers, and feedstock is selected regardless of emissions or the selection of coal. When EI is constrained, there is a significantly larger number of heat exchangers owing to TAC being an unconstrained variable, so the solver did not select coal due to its relatively higher carbon emissions potential. In the 3rd scenario, the model attempts to simultaneously trade-off both objectives and achieves relatively higher TAC and EI values than the individual minimums. In the scenario, the polygeneration hub produces 48.7 kg/s of HPS of which 1.8 kg/s is desuperheated and fed to the HEN whilst 46.9 kg/s is fed to the turbines. 34.2 kg/s and 12.3 kg/s emerge as MPS and LPS from the turbines. These streams are desuperheated and all the MPS is fed to the HEN whilst 7.8 kg/s and 4.9 kg/s of LPS is fed to the HEN and ARS. A total of 15,250 kW of power is produced by the turbines, 9,300 kW is purchased and there is an excess of 2,700 kW. In the ARS, 2.7 kg/s of cooling water at 6.5 °C is produced. The ARS units have heat loads of 53.6 kW, 13.2 kW, 56.0 kW, and 42.3 kW for the absorber, solution heat exchanger, generator, and condenser, giving the ARS a coefficient of performance of 0.714. For the HEN, 17 heat exchangers are selected over 6 temperature intervals, with 7 hot utility exchangers, 8 process heat exchangers, and 2 cold utility exchangers.

5. Conclusions

A systematic integration of renewable and non-renewable energy sources with a polygeneration hub and HEN of a process plant has been presented in this paper. By linking a combined heat and power generation hub to a renewable and non-renewable energy supply chain network, the study demonstrates the capability to provide multiple utility services. This approach not only supplies electricity but also harnesses the steam generated in the boiler to deliver heating, enhancing energy efficiency. The study highlights the utilisation of excess steam to power an absorption refrigeration system, maximising the overall energy utilisation and reducing environmental impact. The integrated network is illustrated as a superstructure with a detailed consideration of transport and energy generation-related emissions and the associated costs of installation and operation. In addition, the superstructure accounts for the seasonal availability of feedstocks and their associated season-dependent prices. The use of the weighted method to simultaneously optimise TAC and EI demonstrated important tradeoffs between cost and emissions. From the case study, combined capital costs for the power generation and transport network infrastructure were the highest, leading to TAC ranging close to a billion dollars. To expedite the transition to renewables, it may be necessary to implement modifications on existing infrastructure, where possible, to minimise capital investment costs. Government policy mediation, such as rebates for installation and use of renewable energy technologies, would also aid the transition. In future studies, costs associated with the transportation of energy between the 2^{nd} and 3^{rd} layers of the superstructure will be considered for pipes, pumps, and electric cables. In addition, a set of condensers may need to be incorporated into the model to account for the ultimate recycling of the steam to the boiler feed. Another important addition to this study would be a sensitivity analysis to investigate the various effects of critical variables and parameters involved.

Acknowledgments

T.B. Chitsiga acknowledges the support of the Mastercard Foundation Scholars Program at the University of Cape Town. Prof A.J. Isafiade acknowledges the support of the National Research Foundation of South Africa (Grant number: 119140) and the Research Office at the University of Cape Town.

References

Cowen N., Vogel A., Isafiade A.J., Čuček L., Kravanja Z., 2019, Synthesis of combined heat exchange network and utility supply chain, Chemical Engineering Transactions, 76, 391 – 396.

DiPippo R., 2008, Geothermal Power Generating Systems, In Geothermal Power Plants. Elsevier, DOI: 10.1016/B978-075068620-4.50009-5.

Florides G. A., Kalogirou S. A., Tassou S. A., Wrobel L. C., 2003, Design and construction of a LiBr-water absorption machine, Energy Conversion and Management, 44(15), 2483–2508, DOI: 10.1016/S0196-8904(03)00006-2.

GAMS Development Corporation, 2015, General Algebraic Modelling System (GAMS), Release 24.4.6, Fairfax, Virginia, USA.

IFEU, 2008, EcoTransIT: Ecological transport information tool, environmental methodology and data, IFEU <ecotransit.org/download/EcoTransIT_World_Methodology_Data_100521.pdf> accessed 28.04.2023.

Isafiade A.J., Short M., 2022, Multi-Objective Optimisation of Integrated Renewable Energy Feedstock Supply Chain and Work-Heat Exchanger Network Synthesis Considering Economics and Environmental Impact, Chemical Engineering Transactions, 94, 1123-1128, DOI: 10.3303/CET2294187.

Isafiade A.J., Cowen N., Vogel A., Čuček L., Kravanja Z., 2022, Synthesis of utility supply chain network and industrial symbioses for heat integration, Journal of Cleaner Production, 380, 134921.

Sun X., Liu L., Sheng Y., Zhang L., Du, J., 2019, Heat exchanger network synthesis with absorption refrigeration cycle integrated considering the optimisation of operating condition, Chemical Engineering Transactions, 76, 301–306, DOI: 10.3303/CET1976051.

Towler G., Sinnott R., 2022, Chemical Engineering Design: Principles, Practice and Economics of Plant and Process Design, 3rd Edition, Elsevier, Oxford, UK.

Wen L., 2020, Model of thermal power plant considering water spray desuperheater for power system analysis, Journal of Physics: Conference Series, 1633(1), 012029, DOI: 10.1088/1742-6596/1633/1/012029.

Xu J., Chen Y., Wang J., Lund P. D., Wang, D., 2022, Ideal scheme selection of an integrated conventional and renewable energy system combining multi-objective optimisation and matching performance analysis. Energy Conversion and Management, 251, 114989, DOI: 10.1016/j.enconman.2021.114989.